

pits were not all active at the same time. The radiocarbon dates associated with Rancholabrean fossils suggest accumulation at least as late as $12,650 \pm 160$ years B.P. (3). Shells have been found previously in one pit but they were associated with Indian artifacts (14), one of which has been dated by radiocarbon methods as 4450 ± 200 years B.P. (2). These shells clearly represent an occurrence entirely distinct from the fossils at the Mutual Benefit site.

The high sea level that accompanied the late Pleistocene marine biozone appears to represent the Sangamonian Interglacial. Therefore, the vertebrate-bearing beds associated with the subsequent lowered sea level may be entirely of Wisconsin age or younger.

JAMES W. VALENTINE
JERE H. LIPPS

Department of Geology and
Institute of Ecology,
University of California, Davis 95616

References and Notes

1. D. E. Savage, *Univ. Calif. Publ. Geol. Sci.* **28**, 215 (1951).
2. H. Howard, *Science* **131**, 712 (1960).
3. T. Y. Ho and L. F. Marcus, *ibid.* **164**, 1051 (1969).

4. R. Berger and W. F. Libby, *Radiocarbon* **8**, 467 (1966); E. S. Deevey, L. J. Gralenski, V. Hoffren, *ibid.* **1**, 144 (1959); C. L. Hubbs, G. S. Bien, H. E. Seuss, *ibid.* **2**, 197 (1960); R. Berger and W. F. Libby, *ibid.* **10**, 402 (1968); R. Berger, A. G. Horney, W. F. Libby, *Science* **144**, 999 (1964); M. A. Tamers and F. J. Pearson, Jr., *Nature* **208**, 1053 (1965).
5. Subsurface compilations have been made by G. D. Woodard from borings by L. T. Evans.
6. E. D. Wilson, personal communication.
7. R. Arnold, *Mem. Calif. Acad. Sci.* **3**, 1 (1903); U. S. Grant and H. R. Gale, *Mem. San Diego Soc. Nat. Hist.* **1**, 1 (1931); J. W. Valentine, *Univ. Calif. Publ. Geol. Sci.* **34**, 309 (1961).
8. W. P. Woodring, M. N. Bramlette, W. S. W. Kew, *U.S. Geol. Surv. Prof. Paper* **207**, 1 (1946).
9. F. P. Fanale and O. A. Schaeffer, *Science* **148**, 312 (1965).
10. H. H. Veeh and J. W. Valentine, *Bull. Geol. Soc. Amer.* **78**, 547 (1967).
11. J. W. Valentine and H. H. Veeh, *ibid.* **80**, 1415 (1969).
12. For a general account of the vertebrates see C. R. Stock, *Los Angeles County Mus. Sci. Ser. No. 4 Paleontol. No. 4* (1956).
13. L. R. Marcus, *Los Angeles County Mus. Contrib. in Sci. No. 38* (1960).
14. A. Woodward, *Bull. So. Calif. Acad. Sci.* **36**, 41 (1937).
15. We thank E. C. Wilson, G. J. Miller, and T. Downs, Los Angeles County Museum of Natural History, for making the fossils available, for arranging site visits, and for numerous other courtesies. Professor G. D. Woodard (Sonoma State College) provided information on the stratigraphic context of the fossils in advance of publication of his geological study.

20 April 1970

Lunar Atmosphere as a Source of Argon-40 and Other Lunar Surface Elements

Abstract. *The lunar atmosphere is the likely source of excess argon-40 in lunar surface material; about 8.5 percent of the argon-40 released into the lunar atmosphere will be implanted in the surface material by photoionization and subsequent interaction with fields in the solar wind. The atmosphere is also likely to be the source of other unexpected surface elements or of solar wind elements that impact from non-solar wind directions.*

Analysis of the lunar samples from Apollo 11 indicates anomalous compositions for several elements. In particular, the isotope ^{40}Ar is overabundant as compared with ^{36}Ar in the fine-grain samples, the ratio being much greater than that expected in the solar wind composition (1) and several times greater than could be accounted for by in situ decay of ^{40}K (2). Heymann *et al.* (3) have shown that the ^{40}Ar is surface correlated and have suggested a lunar source: the ^{40}Ar , produced in the moon by potassium decay, subsequently diffuses into the lunar atmosphere and is then driven back into the surface, perhaps by collisions with the solar wind ions (4).

We show here that the source of ^{40}Ar , and perhaps other surface-correlated elements, is very likely the lunar

atmosphere; the atmospheric argon is ionized and swept into the moon by solar wind fields. However, in the lunar rest frame, the ion is accelerated primarily by the interplanetary electric field, and the resulting flux is not in the direction of the solar wind flow, as has usually been thought, but rather is

Table 1. Orbit parameters for ^{40}Ar starting at one scale height above the lunar surface (calculated for the noon-midnight meridian plane).

λ_1 (deg)	λ_2 (deg)	α (deg)	$\mathcal{E}_{\text{impact}}$ (ev)
-90	-90.0	92.2	215
-60	-59.1	61.4	246
-30	-27.3	30.3	422
-10.4	0	5.5	1390
-9.3	6.5	0	2085

nearly perpendicular to that flow (5). In addition, we show that the energy of the lunar ion will be sufficient for implantation and that the process is reasonably efficient.

The idea that the magnetic field moving with the solar wind can cause lunar ions to impinge upon the surface is not new; Michel (6) has discussed the deposition of ions on the surface due to the solar wind interaction, and recently a representative cycloidal trajectory and impact energy has been calculated (7). These considerations were recalled by T. Gold at the Apollo 11 Lunar Science Conference, Houston (1970).

The source of ^{40}Ar in the lunar atmosphere would be the decay of potassium in the moon to ^{40}Ar , which either diffuses steadily into the lunar atmosphere or which, in the past, has been driven out by some heating of the surface. Once out of the moon, the neutral argon is gravitationally bound and forms part of the equilibrium atmosphere whose density decreases approximately exponentially with a scale height given by

$$h = kT/mg \quad (1)$$

where k is the Boltzmann constant, T and m are the species temperature and mass, and g is the lunar gravitational constant. The ^{40}Ar scale height is about 50 km on the sunlit hemisphere, and about one-third of the argon is at heights greater than h . Previous reviews of the source and loss mechanisms in the lunar atmosphere include discussions of ^{40}Ar in the lunar atmosphere due to decay of ^{40}K in the moon (8) and calculations of atmospheric lifetimes against ionization of $\sim 10^7$ seconds (0.3 year) as compared with 10^8 years of gravitational escape (6).

Whether an ion, once formed, escapes or is accreted will be determined primarily by electric fields at the lunar surface and in the interplanetary medium (5). The interaction of lunar ions with the solar wind is best treated in a frame of reference that is at rest with respect to the moon. In this system there is an interplanetary electric field given by

$$\mathbf{E}_{\text{sw}} = -\mathbf{V}_{\text{sw}} \times \mathbf{B}_{\text{sw}} \quad (2)$$

where \mathbf{V}_{sw} , \mathbf{B}_{sw} , and \mathbf{E}_{sw} are, respectively, the solar wind velocity, magnetic field, and electric field. In addition, the lunar surface electric field will moderate incoming ion energies; this surface potential could have a significant effect

for some locations on the moon. However, the surface field is confined to the lunar plasma sheath which, above the sunlit lunar surface, has a thickness of tens of meters when the moon is in the solar wind; for the purposes of this report, we will discuss only acceleration by the interplanetary electric field.

For simplicity, we assume that \mathbf{V}_{sw} , \mathbf{B}_{sw} , and \mathbf{E}_{sw} are perpendicular. In the crossed electric and magnetic fields, the orbit of an ion formed at rest at $x=y=0$ is an ordinary cycloid given by

$$x = -V_{sw}/\omega_c \sin \omega_c t + V_{sw}t \quad (3)$$

and

$$y = V_{sw}/\omega_c (1 - \cos \omega_c t) \quad (4)$$

where ω_c is the angular cyclotron frequency. The electrostatic force exceeds the gravitational force by a factor $eE_{sw}/mg_{moon} = 5 \times 10^3$; thus gravity becomes a negligible perturbation. The initial motion of an ion is along \mathbf{E}_{sw} , and, as the ion gains energy, the magnetic force curves the ion trajectory in the direction of the solar wind flow, with a resulting cycloidal orbit. The height of the cycloid is $2a_c$, where $a_c = V_{sw}/\omega_c$ is the cyclotron radius of ions released in the lunar rest frame. For ^{40}Ar in a magnetic field of $B_{sw} = 10 \gamma$, a_c is 17,820 km, or about ten lunar radii. Thus, for heavy ions like argon, the cycloidal dimensions are much greater than the lunar radius; the ion's trajectory from formation to impact is the initial part of a cycloid, and the motion is nearly parallel to \mathbf{E}_{sw} . Consequently, most of the flux of lunar ions to the surface is in a direction perpendicular to the solar wind flow. In general, ions formed in the lower sunlit atmosphere are driven up (with respect to \mathbf{E}_{sw}) into the moon, whereas ions formed at the equator and in the upper hemisphere escape. Depending upon the direction of \mathbf{B}_{sw} , the interplanetary electric field is generally upward or downward out of the solar ecliptic plane; and, when the direction of \mathbf{B}_{sw} reverses several times during each solar rotation, the direction of \mathbf{E}_{sw} and of the ion flux also reverses. Although the ion flux is generally in the sunlit portion of the upper or lower hemisphere, this distribution will be somewhat smeared, owing to fluctuations of \mathbf{B}_{sw} out of the ecliptic plane.

The energy of the ion at impact is the energy gain along the interplanetary electric field:

$$\mathcal{E} = eE_{sw} y_1 \quad (5)$$

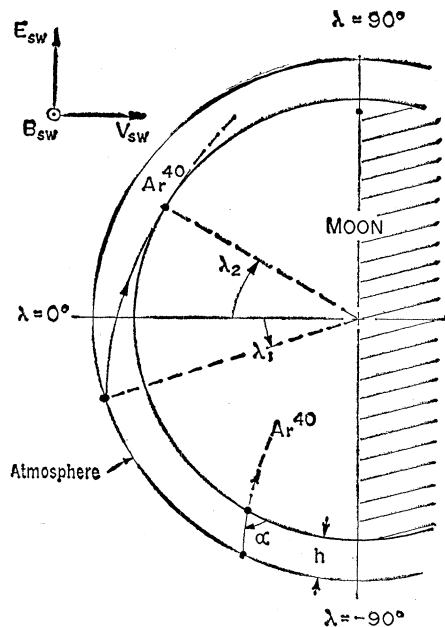


Fig. 1. Sketch of the orbits of ions formed a height h above the surface. An ion formed at λ_1 impacts at λ_2 with an angle α . The "electric" latitude is chosen with respect to the direction of the interplanetary electric field.

where e is the ion charge (we assume single ionization) and y_1 is the y coordinate at impact. The coordinates and other parameters of impact are found by solving the equations for the cycloid with the equation for the locus of the lunar surface. As shown in Fig. 1, an ion formed at some height, say one scale height, above the surface and at an "electric" latitude λ_1 impacts at λ_2 with an impact angle α and an energy \mathcal{E} (the latitude is chosen with respect to the direction of \mathbf{E}_{sw}). There is a critical starting latitude for which an ion just grazes the surface, and ions formed at higher latitudes will escape.

The impact latitude and energy for ^{40}Ar as a function of initial latitude is given in Table 1. About 63 percent of the ions are formed at less than one scale height above the surface, and their impact energies are correspondingly lower. The higher impact energies, of the order of 1 keV, occur near the "electric" equator, which is usually in the vicinity of the lunar equator.

From the calculations shown, it can be seen that most of the ions formed in the lower electric hemisphere, about 40 percent of the total formed, will impinge upon the moon. However, whether an ion is firmly implanted in a lunar grain or is quickly released will depend on the impact energy. Bühler *et al.* (9) found that for argon impinging upon

an aluminum foil, the trapping probability, $\eta_t(\mathcal{E})$, rises linearly to 0.6 at an impact energy \mathcal{E} of 1 keV and levels off to 1 at 3 keV; they expect similar characteristics for silicate grains. We can represent their data as

$$\begin{aligned} \eta_t(\mathcal{E}) &= 0.6 \mathcal{E} & 0 \leq \mathcal{E} \leq 1 \text{ keV} \\ \eta_t(\mathcal{E}) &= 1 - 1.8 \exp(-1.5 \mathcal{E}) & 1 < \mathcal{E} \leq 3 \text{ keV} \\ \eta_t(\mathcal{E}) &= 1 & \mathcal{E} > 3 \text{ keV} \end{aligned} \quad (6)$$

where \mathcal{E} is in kiloelectron volts. The total number of ^{40}Ar atoms that will be trapped can be found by integrating over that volume of the lunar atmosphere whose ions impinge upon the lunar surface. In the integral, the variation in atmospheric density with height and the dependence of impact energy on the height and latitude at which the ion is formed are weighted by the trapping coefficient given in Eq. 6 above.

We thereby calculate that approximately 8.5 percent of the ions that are formed in the atmosphere will be trapped in the surface. Any possible saturation effects are not included in the calculation. It should again be noted that the impact energies and the resulting trapping coefficient are calculated for $B_{sw} = 10 \gamma$. If 5γ were used instead (which may be closer to the average value), then the impact energies would be about half of those tabulated, and perhaps only 5 percent of the ions would be trapped.

From Table 1 we see that the ^{40}Ar impact energies (~ 1 keV) are less than the solar wind ^{36}Ar energy (~ 36 keV); thus we would expect that the ^{40}Ar is not implanted so deeply. This may well be the reason that stepwise heating of lunar samples shows much larger quantities of ^{40}Ar than ^{36}Ar outgassing at low temperatures (10). If most of this ^{40}Ar is lunar and is not contamination from the sample processing, the implication is that the ^{40}Ar flux from the lunar atmosphere exceeds the ^{36}Ar flux from the solar wind. In principle, the $^{40}\text{Ar}/^{36}\text{Ar}$ ratio should also vary with the orientation of an object's surface; ^{36}Ar should be more common in surfaces facing the solar wind, whereas ^{40}Ar should be more common in surfaces parallel to the ecliptic plane. However, this distribution will be somewhat smeared by fluctuations in \mathbf{B}_{sw} (which rotates \mathbf{E}_{sw}), movement of the object, dust transport, and so forth.

Careful analysis of the $^{40}\text{Ar}/^{36}\text{Ar}$ ratio may clarify whether the ^{40}Ar was deposited in large quantities in the past or continuously to the present. It is possible that both the ^{40}Ar and ^{36}Ar fluxes could be used to estimate the length of time a rock fragment has been on the surface and the orientations that it has had. The analysis of returned segments of a Surveyor or a lunar module may determine the present rate of ^{40}Ar deposition and show the expected variation with orientation in the $^{40}\text{Ar}/^{36}\text{Ar}$ ratio.

In conclusion, it appears that the lunar atmosphere is the likely source for the surface-correlated ^{40}Ar in the lunar soil grains. The atmosphere probably contains other elements from the lunar interior and solar wind elements, which have struck the moon and then been released. Thus the lunar atmosphere is likely to be the source of other unexpected surface elements that are not abundant in the solar wind and of solar wind elements that impinge upon the surface from non-solar wind directions.

R. H. MANKA

Space Physics Division,
Manned Spacecraft Center,
Houston, Texas 77058

F. C. MICHEL

Space Science Department,
Rice University,
Houston, Texas 77001

References and Notes

1. Theoretical considerations make a large ^{40}Ar content in the solar wind unlikely [D. D. Clayton, personal communication].
2. K. Marti, G. W. Lugmair, H. C. Urey, *Science* **167**, 548 (1970); J. G. Funkhouser, O. A. Schaeffer, D. D. Bogard, J. Zähringer, *ibid.*, p. 561.
3. D. Heymann, A. Yaniv, J. A. S. Adams, G. E. Fryer, *ibid.*, p. 555.
4. The relationship between the ^{40}Ar data and the lunar atmosphere is discussed in more detail by D. Heymann and A. Yaniv, *Geochim. Cosmochim. Acta*, in press.
5. The energy and flux of lunar ions due to these fields will be described in detail by R. H. Manka and F. C. Michel, in preparation.
6. F. C. Michel, *Planet. Space Sci.* **12**, 1075 (1964).
7. R. H. Manka and H. R. Anderson, *Trans. Amer. Geophys. Union* **50**, 217 (1969).
8. W. Bernstein, R. W. Fredericks, J. L. Vogl, W. A. Fowler, *Icarus* **2**, 233 (1963).
9. F. Bühler, J. Geiss, J. Meister, P. Eberhardt, J. C. Huneke, P. Signer, *Earth Planet. Sci. Lett.* **1**, 249 (1966).
10. R. O. Pepin, L. E. Nyquist, D. Phinney, D. C. Black, *Science* **167**, 550 (1970); D. D. Bogard, personal communication.
11. Supported in part by NASA grant NAS9-5911. We thank Dr. D. D. Clayton (Rice University) and Drs. D. D. Bogard, R. K. Jaggi and C. S. Warren (Manned Spacecraft Center) for helpful discussions; we especially thank Drs. D. Heymann and A. Yaniv (Rice University) for their helpful comments and discussions regarding their data showing the surface correlation of ^{40}Ar .

22 May 1970

Phylum Ectoprocta, Order Cheilostomata: Microprobe Analysis of Calcium, Magnesium, Strontium, and Phosphorus in Skeletons

Abstract. *Calcium, magnesium, and strontium occur in approximately constant ratios in traverses through skeletal walls of a single mineralogy (either calcite or aragonite). Skeletal walls of more than one mineralogy have the magnesium-rich layer (calcite) surrounding the living chamber and the strontium-rich layer (aragonite) on the outside. In contrast, phosphorus may be present in greater or lesser amounts in different parts of the same calcite skeletal wall. Aragonitic crystallites appear oriented roughly perpendicular to skeletal walls, whereas calcitic crystallites are parallel to skeletal walls.*

The phylum Ectoprocta (Bryozoa in part) includes 20,000 living and extinct species (1) and ranks as one of the more diverse groups of organisms. They are abundant in most encrusting communities. The colonies are composed of compartmentalized calcareous skeletons (Figs. 1 and 2) each of which houses a feeding polypide.

Chemical analyses, x-ray diffraction studies, and other techniques have disclosed general characteristics of elemental composition and mineralogy of the skeleton (2, 3). These results are most often expressed as average percentages of different elements or mineral phases. The spatial distribution of mineral phases has been observed to date by staining techniques, optical examination of thin sections, and bulk x-ray diffraction of specimens at different ontogenetic stages (4, 5). Greater precision and flexibility in choice of materials for determining the spatial distribution of calcite and aragonite is permitted by monitoring Sr and Mg by the electron probe in traverses of skeletal walls (Figs. 1-3). Strontium oxide (SrO) is much higher in aragonite than in calcite [1 compared to 0.3 percent (by weight) of ash], whereas MgO is an order of magnitude higher in calcite than in aragonite [3 to 4 compared to 0.3 percent (by weight) of ash] (2). Sr and Mg substitute for Ca in carbonates.

Two types of analysis were made with an ARL-SEM electron probe. (i) Qualitative mechanical, motor-driven traverses (16 $\mu\text{m}/\text{min}$) were made under a static beam which monitored the intensity of Ca, Mg, Sr (four species), and P (1 species) across skeletal walls of several individuals. The samples had been analyzed for their gross elemental and mineralogic composition (2, 6). The probe was operated at 20 kv and a 0.05- μa specimen current. (ii) A few scanning pictures were taken of Ca, Mg, Sr, and P distributions in

order to map these elements in the surface area of transverse or deep tangential sections (Figs. 1-3).

The cuticular layer between calcareous walls of adjacent individuals (Fig. 2) is represented in traverses by a sharp drop in elemental concentration (best seen in Ca, Fig. 4, a, b, and e). This layer is sufficiently thin in some lateral walls so that averaging effects of the probe (over 4 to 5 μm) obscure its recognition. No definite cuticle was observed in adjacent end walls. This supports the observations that lateral walls are generally double calcified walls and that end walls are single calcified walls (7), and consequently that the mode of formation of these walls is quite different (7).

In species of single mineralogy (Fig. 4, species A and D), no significant spatial differences were found within a colony in ratios of Ca, Mg, or Sr. These elements vary to an important extent only with respect to the degree of mineralization and the type of mineralogy (calcite in species A, and aragonite in species D). However, P may vary considerably in amount in adjacent walls (Figs. 4, a and b). Colonies of species A are organized so that adjacent individuals only partly overlap (as in Fig. 2B). During growth, the early-formed part of a lateral wall is against a completely budded individual, and the later-formed part is adjacent to an incompletely budded individual. The high values for P seem to occur only in the early-formed part of the lateral wall. Thus P may be systematically enhanced and depressed in different growth stages of the same individual.

The structure of the calcified wall can be correlated with mineralogy. Species D is aragonitic, and its walls are composed of fibrils of mineral that appear to be perpendicular to, or radiating from the depositional surface. This was observed as "fans" of crys-